May 2015

Mathematical Modeling of Slinky Geothermal Heat Systems

Kyle Hao Chen
Worcester Polytechnic Institute

On Mathematical Modeling of Slinky Geothermal Heat Systems

A Major Qualifying Project
submitted to the Faculty of
WORCESTER POLYTECHNIC INSTITUTE
in partial fulfillment of the requirements for the Degree of Bachelor of Science by

---

by Kyle Hao Chen

Mathematical Sciences
Class of 2015

Advisor: Professor Burt Tilley

Abstract

The purpose of this project was to mathematically model a Slinky-Coil Geothermal Heating System. We first consider and discuss the difficulties of modeling one loop of a slinky coil. We then reduce the problem further to analyzing a half-loop, through non-dimensionalization, separation of variables, eigenfunction expansions, and perturbation series to obtain a function to model the temperature of the slinky coil. In both cases, we examine the quasi-steady approximation, which gives us a steady-state solution to our problem. Our model can successfully model the temperature rise, but it is very inefficient as it requires a very large amount of loops, on the order of thousands, to sustain the ambient temperature of the soil.

Acknowledgements

I would like to thank my family and friends for their neverending support. Without them, I would not be here. Additionally to my teachers and professors, you have taught me how to execute my abilities to the furthest degree. I wish to follow your footsteps as I continue my lifelong dream of becoming a math teacher. I humbly thank each and every one of you.

I must finally thank my advisor for this project, Professor Burt Tilley, for his unwavering patience he had with me during the first three and a quarter terms. I truly deserved none as I was conquering my faults of procrastinating and not asking for help when I needed to. Once I buried my faults, our relationship as I worked on this project evolved from professor and student to partners trying to figure out what our next best plan of attack was. Working through this project with him has been my most valuable experience as a student. I have come to realize that this only comes to those who know how to do the work, read the literature, and most importantly, ask for help. To Professor Tilley, my sincerest thanks.

Contents

List of Figures

Chapter 1

Introduction

1.1 Background

Currently, there is an overreliance on the use of fossil fuels, which has led to a gradual, continuous rise in carbon emissions. The graph below from the Energy Information Agency (EIA) indicates that daily net oil use is projected to be at 72 percent in 2040, which enumerates to between 18 and 19 million barrels of fuel. In 2012, about 92 percent of residential and commercial buildings use energy sources that produce carbon emissions, compared to just 8 percent that use renewable energy. According to the EIA, the 92 percent energy consumption equates to about 8.832 quadrillion BTU[5]. This has led to a general trend towards alternative heating sources.

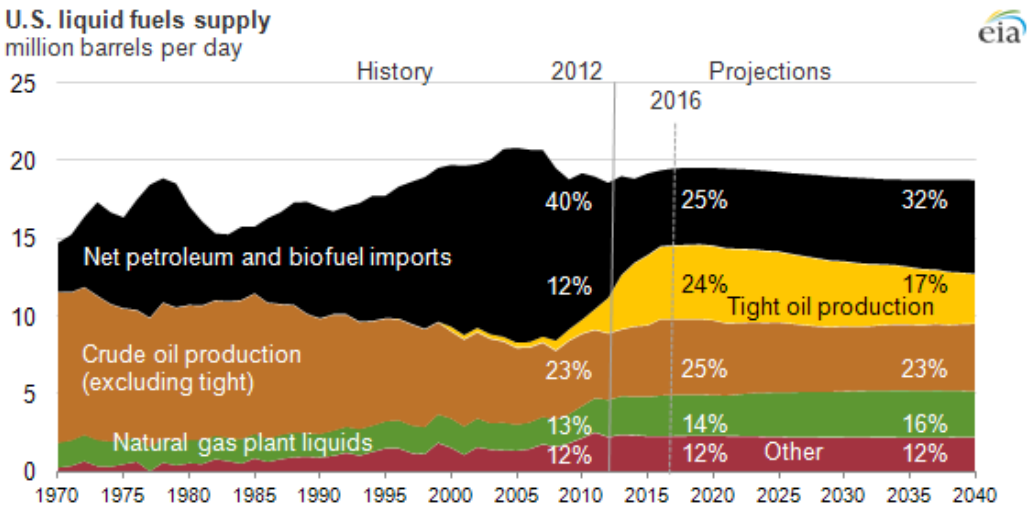

Figure 1.1: United States Daily Use of Fuel[1]

There are some renewable energy sources already in use. One source is Wind Power, where wind turbines harness wind energy via their blades; the kinect energy of the spinning blades is subsequently converted into electrical energy. Areas where wind power is harnessed in large quantities is referred to as a Wind Farm. One major advantage of wind farms is that the wind turbines take up less space on the ground, referred to as low surface footprint. Additionally, wind turbines are low cost in both maintenance and production[6]. There are, however, major downsides to using wind power. The source is intermittent, meaning that wind is not always readily available. Additionally, turbines produce a high level of noise, meaning it is not suited for use in urban areas. One other major downside is its threat to wildlife: airborne animals such as birds can damage the spinning blades and subsequently die from the collision.

Another renewable energy source is Solar Energy, which is energy harnessed by the sun's rays via solar panels. Unlike wind turbines, solar panels generate little noise. Additionally, solar panels are also plentiful, being avaiable around the world[7]. On the contrary, solar panels have high surface footprint due to their size: the towers of wind turbines take up less space on ground from their cylindrical nature, while solar panels

are rectangular "plates" laid at a slight angle with respect to the ground. Secondly, the materials needed to produce solar panels are extremely expensive. Furthermore, ironically in line with wind power, solar energy is also an intermittent source.

Nuclear Power is energy released from nuclear energy via reactors. Unlike wind and solar energy, nuclear power is readily available as the materials needed are available in high quantities[8]. Furthermore, the energy output of nuclear power is extremely high. However, nuclear power is similar to wind power as it is low cost in maintenance. The downsides to nuclear power are unique: the waste produced is radioactive, harmful to all life. Additionally, there are potentials for radiation emission, known to many during the worst-case scenario of a meltdown.

Geothermal heat is an energy source that comes from the earth's core that is continuously reproduced[9]. For the last thirty years has been used as a low-cost heating source for residential home by the use of geothermal heat pumps which comprise of a unit[10]. The main component of a geothermal heating unit a series of pipes that are placed in trenches dug into nearby soil and act in a loop between the earth and a home.

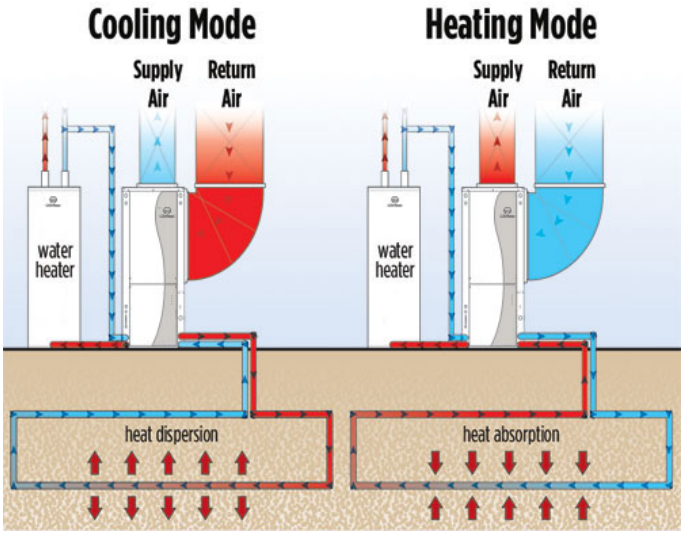

Figure 1.2: Description of Geothermal Heating Unit[2]

Similar to a refrigerator and an air-conditioning unit and as displayed above, the

coolant within the pipes will extract heat from the soil and send it to the home for heating. In order to cool a home, the coolant extracts heat from within the home and then disperses the energy back into the soil. This is possible as soil is warmer in the winter but colder in the summer, which we will mathematically analyze in a later section.

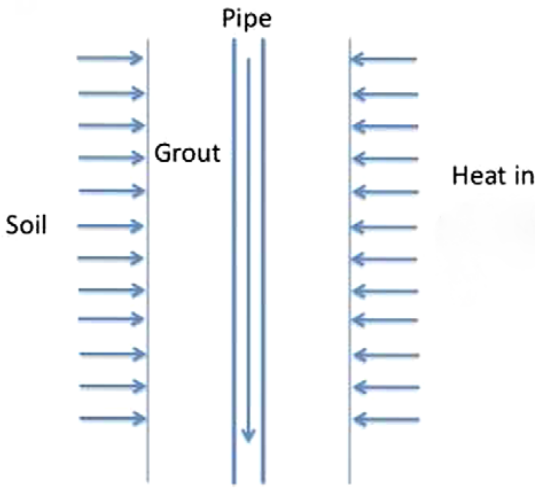

Figure 1.3: Cross section of loop[11]

The required length of the loops depends on the size of the house. We first compute a ratio of time it takes for heat to conduct from soil and how long it takes for a heat pump to heat a home. The former is already known, however, to be very long: the time it takes for heat to diffuse from soil to pipe is on the order of hours:

$$\text{Conduction Time} = \frac{a^2}{\kappa_g} \tag{1.1}$$

where a is the radius of the pipe and κ_g is the thermal diffusivity of the grout. Additionally, we already know that it takes just minutes for heat pumps to achieve the temperature the system is set to:

$$\text{Cycle Time} = \frac{a}{V} \tag{1.2}$$

If we take a ratio of these two time cycles, we find that

$$\frac{\text{Cycle Time}}{\text{Conduction Time}} = \frac{a\kappa_g}{a^2 V} = \frac{\kappa}{Pe} \ll 1 \tag{1.3}$$

where κ is the ratio of thermal diffusivities of grout to fluid (κ_g/κ_f) and

$$Pe = \frac{aV}{\kappa_f} \tag{1.4}$$

is the Péclet number of the fluid flow. We already know that $\kappa = O(1)$, so the Pe is going to be a very large number.

Our next task is to analyze a geothermal pipe with a fixed small radius (about 1 to 2 centimeters[11]) and arbitrary length L. The energy it will be able to absorb in heating mode depends on how fast energy can diffuse from the soil. The power output of a pipe based on work from Ortan et. al.[11] is

$$\text{Power}_{\text{out}} \approx \rho_f c_{pf} V A \Delta T \tag{1.5}$$

where ρ_f represents the mass density of the fluid, c_{pf} represents the specific heat of the fluid, V represents the characteristic fluid velocity, A represents the pipe's cross-sectional area, and ΔT represents the temperature change.

We next calculate the power that feeds into the pipe, which is approximately the product of temperature change, the reciprocal of the conduction time as previously derived, and the surface area of the pipe (disregarding the ends). However, we replace κ_g in the conduction time with k_g as we are concerned with how much heat the grout will conduct (k represents thermal conductivity):

$$\text{Power}_{\text{in}} \approx \big(2\pi a\big) L \frac{\Delta T}{a} k_g \tag{1.6}$$

We next assume that the power intake is approximately the power output in order to solve for L:

$$\begin{aligned} \text{Power}_{\text{in}} &\approx \text{Power}_{\text{out}} \\ (2\pi a) L \frac{\Delta T}{a} k_g &\approx \rho_f c_{pf} V (\pi a^2) \Delta T \\ L &\approx \frac{\rho_f c_{pf} V a^2}{2 k_g} \\ &\approx \frac{\rho_f c_{pf} a V}{k_f} \cdot \frac{k_f}{k_g} \cdot \frac{a}{2} \\ &\approx \frac{a}{2} \cdot \frac{Pe}{k} \end{aligned} \tag{1.7}$$

This means that L is going to be a very large number. The lengths of the pipes are therefore long, usually rounding out at about a few hundred feet.

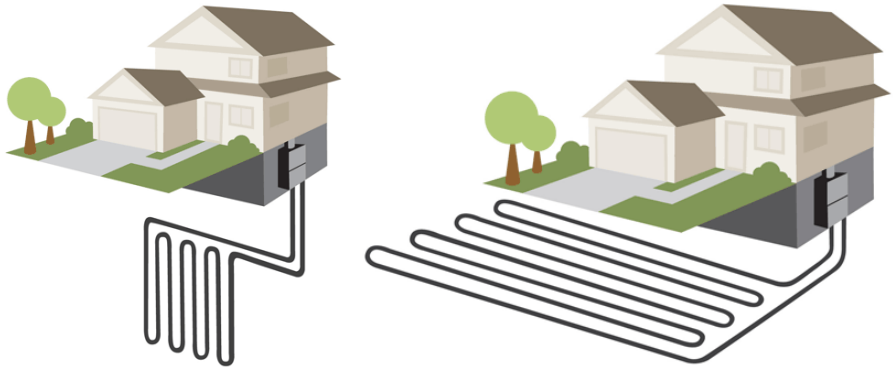

Figure 1.4: A Vertical (Left) and Horizontal (Right) Geothermal Heating System[3]

There are several types of geothermal heating systems based on the arrangements of the loops. In a vertical system, the pipes are buried in large boreholes perpendicular to the surface. The cost to drill the boreholes is quite expensive (especially in regions where the soil is rocky). Compounded with the required length of pipes, installation costs can rise over $20,000. A major benefit in vertical systems, however, is the low footprint since the loops are only placed about 20 feet apart.

In contrast to vertical systems, horizontal systems have the loops buried in shallow

trenches parallel to the surface. As a result, the costs to dig the trenches are significantly lower compared to vertical. However, the length of the pipes will lead to a much larger surface footprint: the loops in a horizontal systems are usually about 200 feet long, which creates a large surface area when laid parallel to the surface.

Figure 1.5: An example of a slinky coil[4]

In a slinky coil, the pipes are coiled similarly to the children's toy of the same name. Slinky systems serve as a compromise of both vertical and horizontal: the length of the pipes are coiled together, so the surface footprint is not nearly as large as that of horizontal. Additionally, the trenches where the pipes are buried are shallow to avoid digging deep. Thus, the cost for installation will be lower compared to both vertical and horizontal.

The purpose of this report is to analyze and model the slinky coil. From there, we will analyze how much more efficient it is compared to vertical and horizontal to see if it is actually cost-effective in the long run.

1.2 Review of Previous Literature

Some research on these problems include the work by Dobson in 1991[12]. The report considered the cooling performance of vertical U-tube ground-coupled heat pumps (GHCPs). Dobson's mathematical model relied on work previously established by Inger-

soll and Plass in 1949. There were also nine assumptions in the model formulation, one of which was that the convection coefficient and all thermal properties were constant. The usage of a numerical model to predict the transient performance proved successful against field data for a 5 day period during the preceding September, with experimental data compiled during the 1990 cooling season.

Zeng et. al. found in 2003 that double U-tube boreholes were superior to single U-tube boreholes with reduction in borehole resistance of 30% - 90%[13]. The article notes that previous models failed to consider the thermal resistance among U-tube pipes. During their mathematical modeling formulation, one important assumption they made was that they considered only two dimensions as opposed to three. They also made several assumptions to keep their modelformulation analytically manageable, one of which was the negligence of the heat capacity of the materials inside the borehole. The two distinct configurations of double U-tube boreholes were also considered, each with their own model.

Ortan et. al. conducted further research in 2009[11] on Taylor dispersion effects of heat in the fluid of the pipes in geothermal heating systems. Their model considered a simple pipe encircled concentrically by a ring of grout. Results showed that higher Péclet numbers were associated with Taylor dispersion effects, and that the dispersion in the fluid and thermostat dictate the minimum tubing length needed for efficiency. Additionally, an explicit definition of the axial thermal difference was found in terms of the Péclet number. However, an assumption made found to be invalid during seasonal changes was that the ambient soil temperature was constant.

Research in 2010 conducted by Al-Khoury et. al., produced a numerical model using a finite element modeling technique for the double U-tube borehole heat exchange (BHE), which was validated through experiments[9]. Their process focused on presenting the numerical analysis describing the capability of a BHE model to simulate three-dimensional heat transfer processes such as conduction and convection in a computationally efficient

manner. They note in their introduction that analytical models are efficient and accurate, but limited in describing the geometry and the boundary conditions. On the other hand, numerical models are much more general, but are computationally inefficient. Additionally, geothermal problems require extremely coarse meshes, where the order of the finite elements is around one million.

Tilley et. al. formulated a simple mathematical model in 2012 to describe the steady-state temperature distribution within a staged geothermal well[14]. This model considered the steady-state, axisymmetric temperature profile of a system of staged, conecentric piping in a well. The model notes of the differences in the usage of the Péclet number: smaller Péclet numbers describes slower convection effects with half of the energy dissipating through diffusion as the fluid in the pipes moves from the source to the surface. On the other hand, energy transmission for a 4 km well is around 80% for sufficiently large Péclet numbers. By consequence, higher Péclet numbers led to better efficiency.

Frei et. al. considered two modeling scenarios in 2012 to create a mathematical modeling framework that calculated a characteristic streamwise length based on a number of factors, including the geometry of the system as well asmaterial properties of the system materials[10]. The first case, which considered the steady-state temperature profiles in the annular fluid region with radial thermal resistance between fluid and soil fixed, found that characteristic length is determined by the smallest eigenvalue of the separable thermal problem, which meant no thermal transport between the core of the pipes and the fluid. The second case, which considered the quasi-steady fluid temperature that captured the radial heat transfer from the fluid to the soil, found that the temperature change is reduced over time.

In terms of specific research on the Slinky arrangement, few models were produced prior to 2011 when Fujii et. al. produced one[15]. In addition, the shape of the coils was simplified to a plate-like heat exchanger. To properly adapt this, the thermal conductivity of the pipes needed to be reduced depending on the pitch of the loops due to the smaller

surface area. The model was then validated through field tests using a finite-element simulator, where the field tests were carried out under varying conditions. The article notes on how at the time, Slinkys tended to be over- or undersized, resulting in a lack of knowledge in creating an optimum design.

1.3 Heat Equation Derivation

As mentioned before, the pipes that form the loops of a geothermal heat pump contain fluid that take energy from the soil and transports it to the home during heating mode. During cooling mode, the energy from the home is transported via the fluid in the pipes and is dispersed back into the soil.

1.3.1 1-Dimensional Case

We first assume we are in one dimension and are trying to model temperature in a pipe of radius R. First, we define temperature as a function of z, the position along the pipe, and t, representing time. Additionally, we define the heat flux with the same variables. Let T denote temperature and q denote heat flux. The heat flux is the amount of thermal energy per unit time flowing in a direction across a unit surface area at position z[16].

We first consider the Law of Conservation of Energy. The Law states that the amount of heat that enters a region plus what is generated inside is equal to the amount of heat that leaves plus the amount stored[17].

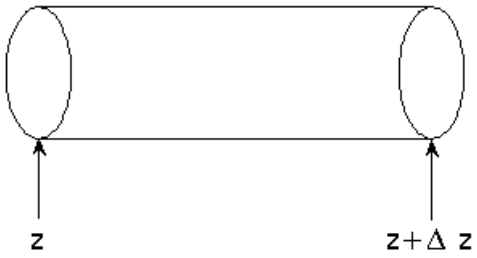

Figure 1.6: Diagram of One-Dimensional Pipe of radius R

If we consider the pipe from position z to $z + \Delta z$, the rate at which heat enters our pipe is $\pi R^2 q(z,t)$ and the rate at which heat leaves is $\pi R^2 q(z + \Delta z, t)$.

The rate of heat storage is proportional to the rate of change of temperature. Assuming ρ to represent the density and c to represent the heat capacity, we aproximate the rate of heat storage by

$$\pi \rho c R^2 \Delta z T_t$$

We next let g represent the generation rate per unit volume. The rate at which heat is generated in the slice is $\pi R^2 \Delta z g$.

We then quantify the law of conservation of energy into the following equation:

$$\pi R^2 q(z,t) + \pi R^2 \Delta z g = \pi R^2 q(z + \Delta z, t) + \pi \rho c R^2 \Delta z T_t \tag{1.8}$$

We can manipulate this equation to arrive at

$$\frac{q(z,t) - q(z + \Delta z, t)}{\Delta z} + g = \rho c T_t \tag{1.9}$$

The ratio on the lefthand-side is a difference quotient. By letting Δz decrease towards zero, we find

$$\frac{q(z,t) - q(z + \Delta z, t)}{\Delta z} = -q_z$$

We apply the same limit process to (1.9) to obtain

$$-q_z + g = \rho c T_t \tag{1.10}$$

There are four qualitative properties of heat flow to consider [16]:

1. If the temperature is constant in a region, no heat energy flows.
2. If there are temperature differences, the heat energy flows from the hotter region to the colder region.
3. The greater the temperature differences (for the same material), the greater the flow of heat energy.
4. The flow of heat energy varies for different materials, even with the same temperature differences.

Mathematician Joseph Fourier summarized these characteristics by stating that the heat flux is equal to the product of thermal conductivity and the negative local temperature gradient. This is now credited as Fourier's Law:

$$q = -k\nabla T \tag{1.11}$$

where k represents the thermal conductivity. Tying this to (1.10) gives us

$$(kT_z)_z + g = \rho c T_t \tag{1.12}$$

If we assume that k, ρ, and c are constants, then we obtain

$$T_{zz} + \frac{g}{k} = \frac{\rho c}{k} T_t$$

Fg is usually considered zero, meaning no heat is generated, so the heat equation in

one-dimension is

$$T_t = \kappa T_{zz} \tag{1.13}$$

where κ, the thermal diffusivity, is $k/\rho c$.

1.3.2 Heat Equation in Multiple Dimensions

Since the pipes in actuality are three-dimensional, we must adapt the heat equation into multiple dimensions. We now assume that the heat flux, q, is a vector denoted as $\overrightarrow{q}$. Recall that in the one-dimensional case, we had

$$-q_z + g = \rho c T_t \tag{1.14}$$

The simple partial derivative will not suffice, as now $\overrightarrow{q}$ is multi-dimensional. To properly account for this, we replace q_z with the divergence of $\overrightarrow{q}$. We also assume once more that $g = 0$.

$$-\nabla \cdot \overrightarrow{q} = \rho c T_t \tag{1.15}$$

However, if apply Fourier's Law,

$$\overrightarrow{q} = -k\nabla T \tag{1.16}$$

we can substitute this relation into (1.15):

$$\rho c T_t = k\nabla \cdot (\nabla T) \tag{1.17}$$

We once more divide both sides by ρc to arrive at

$$T_t = \kappa \nabla^2 T \tag{1.18}$$

1.3.3 Heat Equation with Fluid Flow

We next define the following terms now that we consider fluid flow: Let ρ_f represent the mass density of the fluid (Unit: $\frac{\text{mass}}{\text{volume}}$), c_{pf} represent the specific heat of the fluid (Unit: $\frac{\text{heat energy}}{\text{mass}\cdot\text{temperature}}$), k_f represent the thermal conductivity of the fluid, and V represent the axial fluid velocity (depends only on z). In this case, we assume V to be a constant.

As the pipes in a geothermal heat system will carry or absorb heat, we must also consider convection, the process of heat flowing through a material. To account for this process, we must rewrite our description of our heat flux:

$$\overrightarrow{q} = -k_f \nabla T + \rho_f c_{pf} V T \tag{1.19}$$

We next place this back into (1.10) while once more assuming $g = 0$ to arrive at

$$\rho_f c_{pf} T_t = -\nabla \cdot (-k_f \nabla T + \rho_f c_{pf} V T) \tag{1.20}$$

We then algebraically manipulate our equation to arrive at

$$\rho_f c_{pf} T_t + V \cdot \nabla T = k_f \nabla^2 T - T \nabla \cdot V$$

However, we assumed V to be constant, so the divergence of V will be zero. This gives us

$$\rho_f c_{pf} T_t + V \cdot \nabla T = k_f \nabla^2 T$$

Since our fluid will be flowing with respect to z, we change our above equation to

$$\rho_f c_{pf} [T_t + V T_z] = k_f \nabla^2 T \tag{1.21}$$

We next manipulate this equation by integrating with respect to r from 0 to R. As we

are in cylindrical coordinates, we must first multiply by r before integrating.

$$\begin{aligned}\int_0^R r(\rho_f c_{pf}[T_t + VT_z])\,dr &= \int_0^R rk_f\left[\frac{1}{r}\big(rT_r\big)_r + T_{zz}\right]dr \\ \rho_f c_{pf}\left[\frac{\partial}{\partial t}\int_0^R rT\,dr + V\frac{\partial}{\partial z}\int_0^R rT\,dr\right] &= k_f\left[rT_r\Big|_0^R\right] + k_f\frac{\partial^2}{\partial z^2}\left[\int_0^R rT\,dr\right]\end{aligned}$$

Next define

$$T^* = \frac{1}{R^2}\int_0^R rT(r,z,t)\,dr$$

and let

$$k_f T_r\Big|_{r=R} = q$$

We can then substitute this back into our calculation:

$$\begin{aligned}R^2\big[\rho_f c_{pf}T_t^* + \rho_f c_{pf}VT_z^*\big] &= k_f\big[k_f^{-1}Rq - 0\big] + k_f T_{zz}^* R^2 \\ \rho_f c_{pf}\big[T_t^* + VT_z^*\big] &= k_f T_{zz}^* + R^{-1}q \qquad (1.22)\end{aligned}$$

The above equation is the effective heat equation with fluid flow.

1.4 Soil Temperature Analysis

We discussed earlier that a geothermal heat pump extracts heat from the soil during heating mode and vice versa during cooling mode. To determine whether or not the pipes are efficient in transferring heat, we wish to find the long term behavior of the temperature in the soil with respect to the depth. To model this, we let z represent depth (positive z means below ground) and let T represent temperature. Recall that the heat equation as derived in the previous section for the one-dimensional case is

$$T_t = \kappa T_{zz} \qquad (1.23)$$

with initial conditions

$$T(0,t) = \cos(\omega t) + T_0 \tag{1.24}$$

$$T \to T_0 \quad \text{as} \quad z \to \infty \tag{1.25}$$

where ω represents the seasonal frequency, and T_0 represents the ambient temperature.

Our next assumption is that we assume

$$T = T_0 + u(z)e^{i\omega t} + c.c. \tag{1.26}$$

where $u(z)$ is a function of z and $c.c.$ represents the complex conjugate. We first calculate the derivatives needed:

$$T_t = u(z)(i\omega e^{i\omega t}) + c.c \tag{1.27}$$

$$T_{zz} = u''(z)e^{i\omega t} + c.c. \tag{1.28}$$

We can then substitute these values and solve for u, which we can then use to solve for T:

$$i\omega u(z) = \kappa u''(z) \tag{1.29}$$

$$u(0) = \frac{1}{2} \tag{1.30}$$

$$u \to 0 \quad \text{as} \quad z \to \infty \tag{1.31}$$

The above equation solves into

$$u(z) = Ae^{z\sqrt{\frac{i\omega}{\kappa}}} + Be^{-z\sqrt{\frac{i\omega}{\kappa}}}$$

By our second initial condition for u, $A = 0$. That means that by the first initial

condition, $B = \frac{1}{2}$. We also know that $\sqrt{i} = \frac{1+i}{\sqrt{2}}$, so we can conclude that

$$u = \frac{1}{2} e^{-z(1+i)\sqrt{\frac{\omega}{2\kappa}}} + c.c. \tag{1.32}$$

Therefore, we have an equation for T:

$$T = T_0 + e^{-z(1+i)\sqrt{\frac{\omega}{2\kappa}}} + CC$$

which is equivalent to

$$T = T_0 + e^{-z\sqrt{\frac{\omega}{2\kappa}}} \cos\left[\omega t - z\sqrt{\frac{\omega}{2\kappa}}\right] \tag{1.33}$$

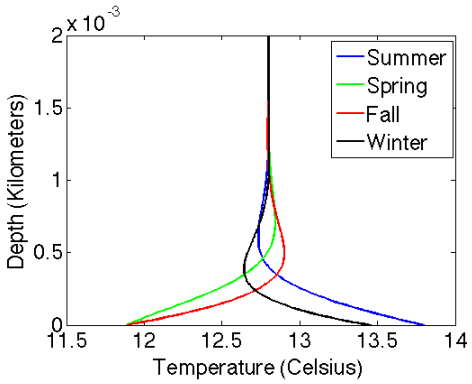

Figure 1.7: Soil Temperature Profile

Above is the annual soil temperature profile with seasonal frequency of 3 months (to model seasons), ambient temperature 12.8° Celsius, and soil thermal diffusitivy of 9.98×10^{-8}[10] square meters per second. Judging from this graph, the soil tends to be cooler in the summer and warmer in the winter. Soil has a low thermal diffusivity, so the time it takes for soil to absorb heat is on the order of months. This charcteristic of soil is what allows wine cellars to work. This is also what allows geothermal heating systems to be efficient: the soil will have the necessary energy to heat the home in the winter, and then vice versa in the summer.

1.5 Sturm-Liouville Theory

1.5.1 Regular Sturm-Liouville Problems

Some of the boundary value problems we will examine in the next chapter will be a regular Sturm-Liouville problem[17], which is given by

$$(s\phi')' - q\phi + \lambda^2 p\phi = 0, \qquad A < x < B \tag{1.34}$$

$$\alpha_1\phi(A) - \alpha_2\phi'(B) = 0 \tag{1.35}$$

$$\beta_1\phi(A) + \beta_2\phi'(B) = 0 \tag{1.36}$$

with the following conditions:

1. $s(x)$, $s'(x)$, $q(x)$, and $p(x)$ are continuous for $A \leq x \leq B$;
2. $s(x) > 0$ and $p(x) > 0$ for $A \leq x \leq B$;
3. The α's and β's are non-negative, and $\alpha_1^2 + \alpha_2^2 > 0$, $\beta_1^2 + \beta_2^2 > 0$
4. The parameter λ occurs only where shown.

The parameter λ is referred to as an eigenvalue, and the corresponding solutions are referred to as eigenfunctions.

Theorem 1. *The regular Sturm-Liouville problem has an infinite number of eigenfunctions ϕ_1, ϕ_2, ..., each corresponding to a different eigenvalue λ_1^2, λ_2^2, ... If $n \neq m$, the eigenfunctions ϕ_n and ϕ_m are orthogonal with weight function $p(x)$:*

$$\int_A^B \phi_n(x)\phi_m(x)p(x)dx = 0, \qquad n \neq m \tag{1.37}$$

1.5.2 Eigenfunction Expansion

Suppose we wish to express a function $f(x)$ defined on the interval $A < x < B$ in terms of the eigenfunctions $\phi_n(x)$ from a regular Sturm-Liouville problem:

$$f(x) = \sum_{n=1}^{\infty} c_n \phi_n(x), \qquad A < x < B \tag{1.38}$$

If we multiply each side by $\phi_m(x)p(x)$ and integrate from A to B, we find

$$\int_A^B f(x)\phi_m(x)p(x)\,dx = \sum_{n=1}^{\infty} c_n \int_A^B \phi_n(x)\phi_m(x)p(x)\,dx \tag{1.39}$$

Recall that Theorem 1 states that the eigenfunctions $\phi_n(x)$ and $\phi_m(x)$ where $n \neq m$ are orthogonal to the weight function $p(x)$. Thus, for the case where $n = m$,

$$\int_A^B f(x)\phi_n(x)p(x)\,dx = c_n \int_A^B \phi_n(x)^2 p(x)\,dx \tag{1.40}$$

Therefore,

$$c_n = \frac{\int_A^B \phi_n(x)^2 p(x)\,dx}{\int_A^B f(x)\phi_n(x)p(x)\,dx} \tag{1.41}$$

This result will allow us to solve boundary value problems with nonhomogenous boundary conditions.

1.6 Overview of Next Chapters

We first discuss the difficulties of modeling the Slinky, and reduce the problem to analyzing a half-loop. By setting up a full boundary-value problem, we apply Separation of Variables and Eigenfunction Expansions to obtain temperature functions, and then compute a perturbation series to determine the temperature rise in the slinky configuration. Once we can compute the temperature rise, we must then determine how many half-loops we need for our model to be efficient.

Chapter 2

Problem Formulation

2.1 Problem Reduction

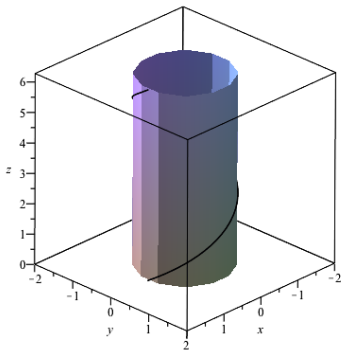

Figure 2.1: Diagram of the 3-dimensional problem

Modeling a full Slinky is extremely difficult, so at first we chose to analyze only one loop in three dimensions. We chose to analyze Laplace's equation in cylindrical coordinates, given by

$$\nabla^2 u = 0 \tag{2.1}$$

where

$$\nabla^2 u = u_{rr} + \frac{1}{r}u_r + \frac{1}{r^2}u_{\theta\theta} + u_{zz}$$

In our model, we analyzed a cylinder of radius a and height h where $h << a$. The region $r < a$ represents soil within the loop and $r > a$ represents soil outside of the loop. To model the temperature outside of the loop, we imposed

$$u(a, \theta, z) = g(\theta, z) \tag{2.2}$$

The problem with this analysis was the lack of definition for g, as we assumed it to be an arbitrary function dependent only on θ and z.

In another analysis, we chose to analyze Laplace's equation in polar coordinates. Thus, we have

$$\nabla^2 u = u_{rr} + \frac{1}{r}u_r + \frac{1}{r^2}u_{\theta\theta}$$

To mimic the loop of a Slinky, we chose to let θ model the temperature by imposing

$$u(1, \theta) = \theta \tag{2.3}$$

We therefore have a simple Dirichlet Problem in a Circle[18] to analyze.

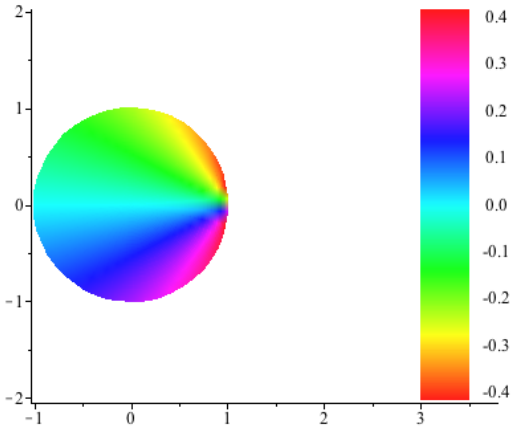

Figure 2.2: Fourier Series Solution

By analyzing the Fourier-Series solution to our problem, we found a noticable discontinuity on the boundary $\theta = 2\pi$. Thus, attempts to model one loop proves difficult.

2.2 Problem Statement

Now suppose we instead look at half of one loop in 2 dimensions.

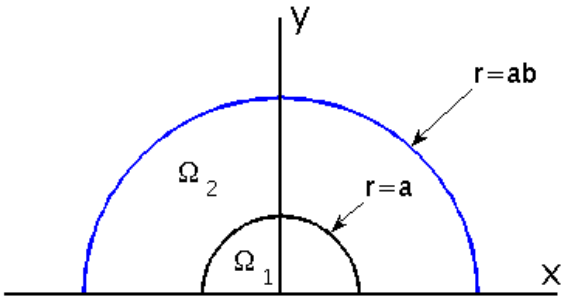

Figure 2.3: Diagram of regions to be analyzed

In order to better analyze a slinky configuration, we instead consider a circle of radius a from $0 \leq \theta \leq \pi$. We also assume there is some other semi-circle of radius ab where $b > 0$. Consider region Ω_1 as $r < a$ and region Ω_2 as $a < r < ab$. Essentially, we choose to look at a semi-circle in two-dimensions to both remove the periodicity problem and any potential discontinuities. In this model, the semi-circle is half of a pipe loop while we let the two described regions be the soil: Ω_1 is the soil within the loop while Ω_2 is the soil outside.

We once again examine the quasi-steady approximation, where all time-derivates are assumed to be zero. This allows us to analyze long-term behavior of a slinky coil, which is one additional aspect we want to analyze.

Mathematically, the standard heat equation is

$$u_t = \kappa \nabla^2 u$$

where u describes temperature and κ is thermal diffusivity. Due to all time-derivatives being zero, however, the equation becomes Laplace's Equation.

Since we are anaylzing two regions, let $u^{(1)}$ and $u^{(2)}$ correspond to Ω_1 and Ω_2, respectively. To fully solve this problem, we must also apply appropriate boundary conditions. We must first assume

$$\lim_{r\to 0} r u_r^{(1)} = 0 \tag{2.4}$$

The are more conditions that need to be stated at $r = a$ (Note: $R > a$). Since we want to build a continuous temperature function, we must assume that the two temperature subfunctions are equivalent at the boundary $r = a$, which we assume to be another function, T, which is dependent on θ:

$$u^{(1)} = u^{(2)} = T(\theta)$$

We also assume the flux to be dependent only on θ and properly relate it to the temprature functions' r-derivatives by applying Fourier's Law:

$$k_s[u_r^{(1)} - u_r^{(2)}] = q(\theta)$$

Finally, since T represents the temperature at our boundary (and thus, the temperature within the pipes), it must obey the heat equation described previously:

$$\rho_f c_{pf}\left[T_t + VT_z\right] = k_f T_{zz} + R^{-1}q$$

However, since the above equation deals with fluid flow in one-dimension, we must better adapt this our model. Since z represented position along the pipe in the one-dimensional case, we use θ here. To mathematically adapt this, we set $z = \theta/a$. Additionally, since

we are dealing with a quasi-steady approximation, $T_t = 0$.

$$\rho_f c_{pf} \frac{V}{a} T_\theta = \frac{k_f}{a^2} T_{\theta\theta} + q$$

So altogether, these descriptions can be written mathematically as

$$u^{(1)} = u^{(2)} = T(\theta) \tag{2.5}$$

$$k_s[u_r^{(1)} - u_r^{(2)}] = q(\theta) \tag{2.6}$$

$$\rho_f c_{pf} \frac{V}{a} T_\theta = \frac{k_f}{a^2} T_{\theta\theta} + q \tag{2.7}$$

Another condition must be added for $r = b$. We assume at that boundary, the temperature is constant:

$$u^{(2)}(ab, \theta) = T_0 \tag{2.8}$$

We must also require θ-conditions to describe the boundaries $\theta = 0$ and $\theta = \pi$. We assume that for $i = 1, 2$, the θ-derivatives are 0:

$$u_\theta^{(i)}(r, \pi) = u_\theta^{(i)}(r, 0) = 0 \tag{2.9}$$

Essentially, our problem is similar to a Dirichlet problem, but with different boundary conditions.

2.3 Non-Dimensionalization

To simplify our problem, we non-dimensionalize the system. Let

$$\bar{r} = \frac{r}{a}, \qquad v(\bar{r}, \theta) = \frac{u(r, \theta)}{T_0}$$

The regions Ω_1 and Ω_2 become $\bar{\Omega}_1$ and $\bar{\Omega}_2$, respectively, with the former describing $\bar{r} < 1$ with temperature function $v^{(1)}$ and the latter describing $\bar{r} > 1$ with temperature function $v^{(2)}$. We originally had

$$\nabla^2 u^{(1)} = 0 \qquad 0 < r < a, \qquad 0 < \theta < \pi \tag{2.10}$$

$$\nabla^2 u^{(2)} = 0 \qquad a < r < ab, \qquad 0 < \theta < \pi \tag{2.11}$$

but these change to

$$\nabla^2 v^{(1)} = 0 \qquad 0 < \bar{r} < 1, \qquad 0 < \theta < \pi \tag{2.12}$$

$$\nabla^2 v^{(2)} = 0 \qquad 1 < r < b, \qquad 0 < \theta < \pi \tag{2.13}$$

The boundary conditions also change. (2.4) changes to

$$\lim_{\bar{r} \to 0} \bar{r} v^{(1)}_{\bar{r}} = 0 \tag{2.14}$$

For our other conditions, (2.5) becomes

$$v^{(1)} = v^{(2)} = \bar{T}(\theta) \tag{2.15}$$

(2.6) becomes

$$v^{(1)}_{\bar{r}} - v^{(2)}_{\bar{r}} = \bar{q}(\theta) \tag{2.16}$$

and (2.7) becomes

$$Pe\bar{T}_\theta = \bar{T}_{\theta\theta} + \bar{q} \tag{2.17}$$

Additionally at $\bar{r} = b$,

$$v^{(2)}(b, \theta) = 1 \tag{2.18}$$

The θ-conditions also change:

$$v_\theta^{(i)}(\bar{r}, 0) = v_\theta^{(i)}(\bar{r}, \pi) = 0 \tag{2.19}$$

2.4 Homogeneous Solution

To solve this, we must first apply separation of variables. Consider Laplace's equation, given by

$$\nabla^2 v = 0$$

where

$$\nabla^2 v = v_{\bar{r}\bar{r}} + \frac{1}{\bar{r}} v_{\bar{r}} + \frac{1}{\bar{r}^2} v_{\theta\theta}$$

Let

$$v = R(r)Q(\theta)$$

If we substitute this back into Laplace's equation, we arrive at

$$RQ + \frac{1}{\bar{r}} RQ + \frac{1}{\bar{r}^2} RQ'' = 0 \tag{2.20}$$

If we divide both sides by v, we find that

$$\frac{R''}{R} + \frac{1}{\bar{r}} \frac{R'}{R} + \frac{1}{\bar{r}^2} \frac{Q''}{Q} = 0 \tag{2.21}$$

We then rearrange the terms to arrive at

$$\bar{r}^2 \frac{R''}{R} + \bar{r} \frac{R'}{R} = -\frac{Q''}{Q} \tag{2.22}$$

Both sides must be equal to some constant λ^2, where λ is an eigenvalue of our problem. We must then determine what each individual equation will solve into. We first analyze the differential equation for Q:

$$-\frac{Q''}{Q} = \lambda^2 \tag{2.23}$$

This simplifies to

$$Q + \lambda^2 Q = 0 \tag{2.24}$$

which then solves into

$$Q(\theta) = A\cos(\lambda\theta) + B\sin(\lambda\theta)$$

Our original function is also π-periodic, so we can conclude that $\lambda = n$. Thus,

$$Q(\theta) = A\cos(n\theta) + B\sin(n\theta)$$

Our next task is to determine A_i and B_i. We know that the θ-derivatives are 0 at $\theta = 0, \pi$. If we compute Q', which is given by

$$Q'(\theta) = -nA\sin(n\theta) + nB\cos(n\theta)$$

We can conclude that $B = 0$. Therefore, our first eigenfunction is

$$Q(\theta) = A\cos(n\theta) \tag{2.25}$$

To solve for our second eigenfunction, we examine

$$\bar{r}^2\frac{R''}{R} + \bar{r}\frac{R'}{R} = n^2 \tag{2.26}$$

This simplifies to

$$\bar{r}^2 R'' + \bar{r}R' - n^2 R = 0 \tag{2.27}$$

This is a Cauchy-Euler equation, whose solutions are of the form $\bar{r}^{\alpha}$[17], where α is an arbitrary constant. If we use this idea, we find that

$$\big(\alpha(\alpha-1)+\alpha-n^2\big)r^{\alpha}=0$$

This means that $\alpha = n$. Thus, in general for $v^{(i)} = R^{(i)}(\bar{r}Q(\theta)$,

$$R^{(i)}(\bar{r}) = C_i\bar{r}^n + D_i\bar{r}^{-n} \tag{2.28}$$

Similarly, we must compute what the remaining constants are. Using (2.14), we can conclude that $D_1 = 0$. Since our original function must be a Fourier Series, we can thus conclude that

$$v^{(1)}(r,\theta) = a_0 + \sum_{n=1}^{\infty} a_n\bar{r}^n\cos(n\theta) \tag{2.29}$$

$$v^{(2)}(r,\theta) = b_0 + c_0\sum_{n=1}^{\infty}\left[b_n\bar{r}^n + c_n\bar{r}^{-n}\right]\cos(n\theta) \tag{2.30}$$

2.5 Eigenfunction Expansion for $v^{(1)}$

Due to the nonhomogenous boundary conditions, we must perform an eigenfunction expansion for $v^{(1)}$ and $v^{(2)}$. As our function depends on two variables, we must decide on which eigenfunction to perform an expansion on. For simplicity, we choose our eigenfunction in θ. Define

$$v^{(1)}(r,\theta) = \sum_{n=0}^{\infty} c_n(\bar{r})cos(n\theta) \tag{2.31}$$

where

$$c_n(\bar{r}) = \frac{\int_0^\pi v^{(1)} \cos n\theta \, d\theta}{\int_0^\pi \cos^2 n\theta \, d\theta} = \frac{2}{\pi} \int_0^\pi v^{(1)} \cos n\theta \, d\theta \tag{2.32}$$

We must then take our original equation (Laplace's Equation), multiply both sides by our eigenfunction, then integrate over θ:

$$0 = \int_0^\pi \cos n\theta \left[\nabla^2 v^{(1)}\right] d\theta \tag{2.33}$$

After some algebraic simplification, we find that we have a second-order ODE for $c_n(\bar{r})$:

$$\bar{r}^2 \frac{d^2}{d\bar{r}^2} c_n(\bar{r}) + \bar{r} \frac{d}{d\bar{r}} c_n(\bar{r}) - n^2 c_n(\bar{r}) = 0 \tag{2.34}$$

which solves into

$$c_n(\bar{r}) = A_n \bar{r}^n + B_n \bar{r}^{-n}$$

However, we can conclude that $B_n = 0$ by (2.14). Therefore

$$c_n(\bar{r}) = A_n \bar{r}^n \tag{2.35}$$

The case where $n = 0$ will give a logarithmic term, but its constant will be 0 due to (2.14). The reason for logarithmic terms is explained in the next section.

2.6 Eigenfunction Expansion for $v^{(2)}$

We apply a similar process where we define

$$d_n(\bar{r}) = \frac{\int_0^\pi v^{(2)} \cos n\theta \, d\theta}{\int_0^\pi \cos^2 n\theta \, d\theta} = \frac{2}{\pi} \int_0^\pi v^{(1)} \cos n\theta \, d\theta \tag{2.36}$$

Based on our results of the homogeneous solution, we find that

$$d_n(\bar{r}) = C_n \bar{r}^n + D_n \bar{r}^{-n} \tag{2.37}$$

However, if we examine our ODE for $d_n(\bar{r})$,

$$\bar{r}^2 \frac{d^2}{d\bar{r}^2} d_n(\bar{r}) + \bar{r} \frac{d}{d\bar{r}} d_n(\bar{r}) - n^2 d_n(\bar{r}) = 0 \tag{2.38}$$

We must also account for the case where $n = 0$. The differential equation here is

$$\bar{r} \frac{d^2}{dr^2} d_0(\bar{r}) + \frac{d}{d\bar{r}} d_0(\bar{r}) = 0 \tag{2.39}$$

We first apply Reduction of Order where

$$y = \frac{d}{d\bar{r}} d_0(\bar{r})$$

The equation to solve becomes

$$\bar{r} y' + y = 0 \tag{2.40}$$

We then apply Separation of Variables to solve this differential equation:

$$\begin{aligned}
\bar{r} y' &= -y \\
\frac{y'}{y} &= -\frac{1}{\bar{r}} \\
\ln y &= -\ln(\bar{r}) \\
y &= \bar{r}^{-1} \\
\frac{d}{d\bar{r}} d_0(\bar{r}) &= \bar{r}^{-1}
\end{aligned}$$

Thus, the solution for this particular case is

$$d_0(\bar{r}) = K_1 \ln(\bar{r}) + K_2 \tag{2.41}$$

2.7 Boundary Conditions for $c_n(\bar{r})$ and $d_n(\bar{r})$

To properly determine $c_n(\bar{r})$ and $d_n(\bar{r})$, we must determine boundary conditions based on those for $v^{(1)}$ and $v^{(2)}$. To do so, we must take the original conditions we set and integrate with respect to θ after mutiplying them by our eigenfunction. If we examine the boundary condition for $\bar{r} = b$, we see

$$v^{(2)}(b, \theta) = 1$$

Multiplying by our eigenfunction $\cos(n\theta)$ and then integrating with respect to θ gives us 0 for $n \neq 0$ and 1 for $n = 0$. Therefore

$$\int_0^\pi v^{(2)}(b, \theta) \cos(n\theta)\, d\theta = \begin{cases} \pi & n = 0 \\ 0 & n \neq 0 \end{cases}$$

But our lefthand-side is equal to $\frac{\pi}{2} d_n(b)$. Thus,

$$d_n(b) = \begin{cases} \dfrac{2}{\pi} & n = 0 \\ 0 & n \neq 0 \end{cases} \tag{2.42}$$

We can then similarly conclude that

$$c_n(1) = d_n(1) = \frac{2}{\pi} \int_0^\pi \bar{T}(\theta) \cos(n\theta)\, d\theta \tag{2.43}$$

By computing the eigenfunction expansion, we find that

$$A_n = \frac{2}{\pi}\int_0^{\pi} \bar{T}(\theta)\cos(n\theta)\,d\theta \tag{2.44}$$

Additionally,

$$C_n + D_n = \frac{2}{\pi}\int_0^{\pi} \bar{T}(\theta)\cos(n\theta)\,d\theta \tag{2.45}$$

But our result from (2.41) shows that we have a logarithmic term for $n = 0$. If we use (2.43), we know that

$$K_2 = \frac{2}{\pi}\int_0^{\pi} \bar{T}(\theta)\,d\theta \tag{2.46}$$

So if we use (2.42), we see that

$$K_1 = \frac{2}{\pi \ln b}\left[1 - \int_0^{\pi} \bar{T}(\theta)\,d\theta\right] \tag{2.47}$$

Also from (2.42), we can say that for $n \neq 0$,

$$C_n\big(b\big)^n + D_n\left(\frac{1}{b}\right)^n = 0 \tag{2.48}$$

Multiplying both sides by b^n gives

$$C_n b^{2n} + D_n = 0 \tag{2.49}$$

Thus, we have

$$D_n = -C_n b^{2n} \tag{2.50}$$

We then substitute this value back into (2.45) to reach

$$C_n\big(1 - b^{2n}\big) = \frac{2}{\pi}\int_0^{\pi} \bar{T}(\theta)\cos(n\theta)\,d\theta$$

Therefore, we have

$$C_n = \frac{2}{\pi(1-b^{2n})}\int_0^\pi \bar{T}(\theta)\cos(n\theta)\,d\theta \tag{2.51}$$

Thus far, we can conclude that

$$v^{(1)}(\bar{r},\theta) = A_0 + \sum_{n=1}^{\infty} A_n \bar{r}^n cos(n\theta) \tag{2.52}$$

where

$$A_n = \frac{2}{\pi}\int_0^\pi \bar{T}(\theta)\cos(n\theta)\,d\theta \tag{2.53}$$

Similarly,

$$v^{(2)}(\bar{r},\theta) = K_1 \ln\bar{r} + A_0 + \sum_{n=1}^{\infty}\left[C_n\bar{r}^n + D_n\bar{r}^{-n}\right]cos(n\theta) \tag{2.54}$$

where

$$K_1 = \frac{2}{\pi \ln b}\left[1 - \int_0^\pi \bar{T}(\theta)\,d\theta\right] \tag{2.55}$$

and for $n \neq 0$,

$$C_n = \frac{2}{\pi(1-b^{2n})}\int_0^\pi \bar{T}(\theta)\cos(n\theta)\,d\theta \tag{2.56}$$

$$D_n = -\frac{2b^{2n}}{\pi(1-b^{2n})}\int_0^\pi \bar{T}(\theta)\cos(n\theta)\,d\theta \tag{2.57}$$

2.8 Regular Perturbation Series for T

The Péclet Number is going to be a very large number, i.e. $Pe \gg 1$, so we next compute a Regular Perturbation Series for T. We let

$$\bar{T} = \bar{T}_0(\theta) + \frac{\bar{T}_1(\theta)}{Pe} + ... \tag{2.58}$$

Next, we set a system of equations to solve:

- $O(1) : -\dfrac{d\bar{T}_0}{d\theta} = 0$
- $O\left(\dfrac{1}{Pe}\right) : -\dfrac{d\bar{T}_1}{d\theta} = -\bar{q} - \dfrac{d^2\bar{T}_0}{d\theta^2}$

If we solve the first system, we find that

$$\bar{T}_0(\theta) = A \tag{2.59}$$

where A is some constant. If we use this idea to solve for our second equation, we find that

$$\begin{aligned} \frac{d\bar{T}_1}{d\theta} &= -\bar{q} - \frac{d^2\bar{T}_0}{d\theta^2} \\ &= -\bar{q} \end{aligned}$$

This solves to

$$\bar{T}_1(\theta) = \int_0^\theta q(\bar{\theta})\, d\bar{\theta} + B \tag{2.60}$$

where B is another arbitrary constant.

Recall that we previously defined q as a Fourier Series:

$$\bar{q} = q_0 + \sum_{n=1}^{\infty} q_n \cos(n\theta)$$

We use this to have an explicit definition for our original pertubation series:

$$\bar{T}(\theta) = A + \frac{1}{Pe}\left[q_0\theta + \sum_{n=1}^{\infty} \frac{q_n}{n} \sin(n\theta)\right] + ... \tag{2.61}$$

Our next task is to determine the terms of q_n. We already know that

$$\int_0^\pi A_0 + q_0 \ln(b)\, d\theta = \int_0^\pi v^{(2)}(b, \theta)\, d\theta = \pi \tag{2.62}$$

Therefore

$$A_0 = 1 - q_0 \ln(b) \tag{2.63}$$

We next assume $q_n = 0$ for $n \neq 0$. Our analysis now only requires us to find q_0. The equation we need is the definition of A_0, which we know to be

$$A_0 = \frac{1}{\pi} \int_0^{\pi} \bar{T}\, d\theta \tag{2.64}$$

We use this to determine that

$$A_0 = A + \frac{\pi q_0}{2Pe} \tag{2.65}$$

We substitute this value into (2.63) to find

$$A + \frac{\pi q_0}{2Pe} = 1 - q_0 \ln(b) \tag{2.66}$$

We thus can manipulate this algebraically to find

$$q_0 = \frac{1 - A}{\ln(b) + \frac{\pi}{2Pe}} = \frac{2Pe[1 - A]}{\pi + 2Pe \ln(b)} \tag{2.67}$$

We substitute this back into our definition of $\bar{T}$ to find

$$\bar{T}(\theta) = A + \frac{2[1 - A]}{\pi + 2Pe \ln(b)}\theta \tag{2.68}$$

Chapter 3

Results

We analyze our results from the last chapter. First, we must set a temperature range for the ambient temperature, which is A. We know that T_0 represented the dimensional ambient temperature, which we assume to be 12.8° Celsius based on our soil temperature profile. We use the ambient soil temperature range assumed from Frei et. al.[10], which is between 10 and 16 Celsius, and adapt that to A:

$$0.78125 < A < 1.25 \tag{3.1}$$

The next is to set a range for the $Pe\ln(b)$. Ortan cites Péclet Numbers to be in the range of[11]:

$$20,000 < Pe < 700,000$$

In our case, we consider $\ln(b)$ to have little effect on the growth of Pe, so we set $Pe\ln(b)$ to be within the same range. Our goal is to model the temperature rise from $\theta = 0$ to $\theta = \pi$. We use our function we obtained at the end of the last chapter to compute $\bar{T}(\pi) - \bar{T}(0)$:

$$\bar{T}(\pi) - \bar{T}(0) = \frac{2\pi[1 - A]}{\pi + 2Pe\ln(b)} \tag{3.2}$$

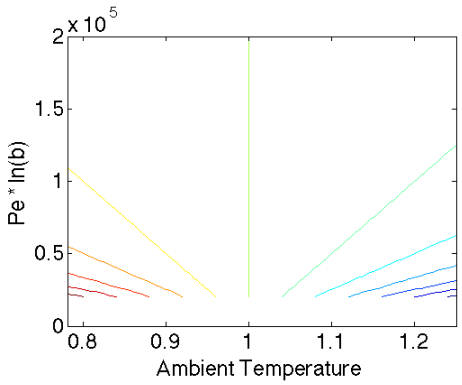

Figure 3.1: Contour Plot of $\bar{T}(\pi) - \bar{T}(0)$

This graph suggests a linear relation in the temperature rise, which is consistent with our results from the last chapter.

We must next analyze the necessary length of piping. To do so, we define a sequence to describe the temperature along our Slinky based on the half-loop model. We set our initial temperature to zero (i.e. $T_0 = 0$) and set

$$T_{i+1} - T_i = \frac{2\pi}{2 + Pe\ln(b)}(1 - T_i) \tag{3.3}$$

Algebraic manipulation of this equation leads to

$$T_{i+1} - 1 = \left[1 - \frac{2\pi}{2 + Pe\ln(b)}\right](T_i - 1) \tag{3.4}$$

We next set

$$\alpha_i = T_i - 1 \tag{3.5}$$

This allows us to determine the temperature ratio:

$$\frac{\alpha_{i+1}}{\alpha_i} = 1 - \frac{2\pi}{2 + Pe\ln(b)} \tag{3.6}$$

If we analyze the terms

$$\alpha_1 = -\left[1 - \frac{2\pi}{2 + Pe\ln(b)}\right]^1 \qquad \alpha_2 = -\left[1 - \frac{2\pi}{2 + Pe\ln(b)}\right]^2$$

This allows us to determine α_i:

$$\alpha_i = -\left[1 - \frac{2\pi}{2 + Pe\ln(b)}\right]^i \tag{3.7}$$

We need to determine for which i such that α_i will converge to the ambient temperature. We let ϵ be an arbitrary positive number (i.e. $\epsilon > 0$) such that

$$|\alpha_i| < \epsilon \tag{3.8}$$

We then substitute our definition of α_i to determine i:

$$\begin{aligned}
\left| -\left[1 - \frac{2\pi}{2 + Pe\ln(b)}\right]^i \right| &< \epsilon \\
\left[1 - \frac{2\pi}{2 + Pe\ln(b)}\right]^i &< \epsilon \\
\ln\left(\left[1 - \frac{2\pi}{2 + Pe\ln(b)}\right]^i\right) &< \ln(\epsilon) \\
i\ln\left(\left[1 - \frac{2\pi}{2 + Pe\ln(b)}\right]\right) &< \ln(\epsilon) \\
i &> \frac{\ln(\epsilon)}{\ln(1 - \frac{2\pi}{2+Pe\ln(b)})} \\
i &> \frac{\ln(\epsilon)}{\ln(2 + Pe\ln(b) - 2\pi) - \ln(2 + Pe\ln(b))}
\end{aligned} \tag{3.9}$$

This is the smallest i for which T_i is going to be within ϵ of 1. Now suppose we let $\epsilon \approx 0.01$ and let $Pe\ln(b) \approx 30,000$, we find that

$$i > \frac{\ln(0.01)}{\ln(.99979)} \approx 21987.23117 \tag{3.10}$$

By analyzing our lower bound for $Pe\ln(b)$, we find that we will need at least 21988 half-loops, or 10994 full loops for our slinky coil to maintain the ambient temperature, i.e. run efficiently.

Chapter 4

Conclusions

Our model proved successful in modeling temperature rise but proved inefficient in design. The large number of half-loops required for efficiency instead suggests that the slinky coil is similar to a plate-like exchanger similar to the model produced by Fujii et. al.[15] With this result, future work may include examining the case where all terms of our Fourier Series describing the heat flux are considered. Another possible extension may include the analysis of the non-quasi-steady approximation by introducing time into our model.

Bibliography

[1] Energy Information Agency. Annual energy outlook 2014. http://www.eia.gov/todayinenergy/detail.cfm?id=14211, 2014.

[2] EnergyHomes.org. What is a geothermal heat pump? http://www.energyhomes.org/renewable%20technology/howgeoworks.html, 2008.

[3] Geothermal Montana. What is a geothermal heat pump? http://www.geothermalmontana.com/what-is-a-geothermal-heat-pump.html.

[4] GeoJerry. Naeem's slinky earth loop installation. http://www.geojerry.com/Naeemsslinkyearthloopinstallation.html, 2014.

[5] Energy Information Agency. Primary energy consumption by source and sector. http://www.eia.gov/totalenergy/data/monthly/pdf/flow/primary_energy.pdf, 2012.

[6] Energy Informative. Wind energy pros and cons. http://energyinformative.org/wind-energy-pros-and-cons/, 2015.

[7] Energy Informative. Solar energy pros and cons. http://energyinformative.org/solar-energy-pros-and-cons/, 2014.

[8] Energy Informative. Nuclear energy pros and cons. http://energyinformative.org/nuclear-energy-pros-and-cons/, 2013.

[9] R. Al-Khoury et. al. Efficient numerical modeling of borehole heat exchangers. *Computers and Geosciences*, 2010.

[10] S. Frei et. al. On thermal resistance in concentric residential geothermal heat exchangers. *J Eng Math*, 2013.

[11] Ortan et. al. On taylor dispersion effects for transient solutions in geothermal heating systems. *Internation Journal of Heat and Mass Transfer*, 2008.

[12] M.K. Dobson. An experimental and analytical study of the transient behavior of vertical u-tube ground-coupled heat pumps in the cooling mode. Technical report, Texas A&M Universities, 1991.

[13] Zeng et. al. Heat transfer analysis of boreholes in vertical ground heat exchangers. *Internation Jornal of Heat and Mass Transfer*, 2003.

[14] B. S. Tilley et. al. On temperature attenuation in staged open-loop wells. *Renewable Energy*, 2012.

[15] Fujii et. al. Numerical modeling of slinky-coil ground heat exchangers. *Geothermics*, 2011.

[16] Richard Habermann. *Elementary Applied Differential Equations, With Fourier Series and Boundary Value Problems.* Prentice Hall, third edition, 1998.

[17] David L. Powers. *Boundary Value Problems and Partial Differential Equations.* Elsevier, Inc., sixth edition, 2010.

[18] Stanley J. Farlow. *Partial Differential Equations for Sciences and Engineers.* Dover Publications, Inc., 1993.